JOC Article

Structure and Absolute Stereochemistry of Phormidolide, a New Toxic Metabolite from the Marine Cyanobacterium *Phormidium* sp.

R. Thomas Williamson,[†] Anna Boulanger,[†] Alexandra Vulpanovici,[‡] Mary A. Roberts,[†] and William H. Gerwick*,[†,‡]

College of Pharmacy, Oregon State University, Corvallis, Oregon 97331, and Department of Biochemistry and Biophysics, Oregon State University, Corvallis, Oregon 97331

bill.gerwick@orst.edu

Received April 5, 2002

The extract from a laboratory culture of an Indonesian isolate of the cyanobacterium *Phormidium* sp. displayed inhibitory activity in a Ras-Raf protein interaction assay. Assay-guided fractionation led to the isolation of both active and inactive materials of novel structure. The major inactive metabolite, phormidolide, was nevertheless highly toxic to brine shrimp ($LC_{50} = 1.5\ \mu M$), and hence, its structure was elucidated using various spectroscopic methods, primarily NMR. A series of partial structures were developed from standard experiments and then assembled using GHMBC, 2D INADEQUATE, and ACCORD-ADEQUATE data obtained on a ^{13}C-enriched sample. The relative stereochemistry at phormidolide's 11 chiral centers was established using the *J*-based configuration analysis method in concert with the G-BIRD$_R$-HSQMBC NMR experiment. Absolute stereochemistry was determined on a bis-acetonide derivative using the variable temperature Mosher ester method. The robust number of NMR restraints provided from determination of most homonuclear and heteronuclear coupling constants in phormidolide, along with an abundance of NOE information, allowed construction of a refined lowest energy three-dimensional structure in Macromodel. Phormidolide is one of only a few macrolide-type natural products to be reported from marine cyanobacteria.

Introduction

Marine cyanobacteria have emerged over the past decade as an extraordinarily rich source of diverse natural products, many of which have extremely potent biological properties.[1] Most of these derive from the combination of polyketide synthase and nonribosomal peptide synthetase biosynthetic pathways. However, a minor theme in the natural products chemistry of these life forms is the production of complex polyketides of relatively large molecular size and a characteristic occurrence of oxygen-containing heterocycles.[2] Moreover, some of these are of relevance to human health issues (e.g., polycavernoside A), being responsible for human intoxications and a few deaths from their incidental ingestion.[3] In this regard, our investigation of a species of *Phormidium* has led to the isolation of a novel bromine-containing macrolide (**1**) that has several interesting biological properties. Moreover, its complex structure with 11 stereocenters has posed a number of challenging questions in the course of structure elucidation, and this has consequently been a superb opportunity for the development and application of new NMR approaches in structure elucidation.

As part of our natural products mechanism-based screening program for new potential anticancer lead compounds, we found the extracts of three cultures of the marine cyanobacterium *Phormidium* sp. to show potent and specific inhibitory activity to Ras-Raf protein−protein interaction.[4] This interaction has been identified as a critical component in the mitogen-activated signal transduction cascade that is upregulated in a number of cancer types and is therefore an attractive site at which to find new inhibitors.[5] At the time of initiating these studies, specific inhibitors of this interaction were unknown other than the consensus sequence of the interacting peptide fragment. Analysis of these *Phormidium* extracts by TLC and NMR showed a single major secondary metabolite to be present in all three isolates. However, Ras-Raf assay guided fractionation led to the isolation of a novel and very minor chlorophyll-type pigment as the active component; its isolation, structure elucidation, and biological properties will be presented elsewhere.[6] Nevertheless, the major component accounted for up to 20% of the extractable lipids in some

* To whom correspondence should be addressed. Tel: 541-737-5801. Fax: 541-737-3999.
[†] College of Pharmacy.
[‡] Department of Biochemistry and Biophysics.

(1) Gerwick, W. H.; Tan, L. T.; Sitachitta, N. In *The Alkaloids*; Cordell, G. A., Ed.; Academic Press: San Diego, 2001; Vol. 57, pp 75−184.
(2) Yasumoto, T.; Murata, M. *Chem. Rev.* **1993**, *93*, 1897−1909.
(3) Yotsu-Yamashita, M.; Haddock, R. L.; Yasumoto, T. *J. Am. Chem. Soc.* **1993**, *115*, 1147−1148.
(4) Finney, R.; Herrera, D. *Methods Enzymol.* **1995**, *255*, 310−323.
(5) Pumigia, K.; Chow, Y. H.; Fabian, J.; Morrison, D.; Decker, S.; Jove, R. *Mol. Cell Biol.* **1995**, *15*, 398−410.

10.1021/jo020240s CCC: $22.00
Published on Web 10/23/2002

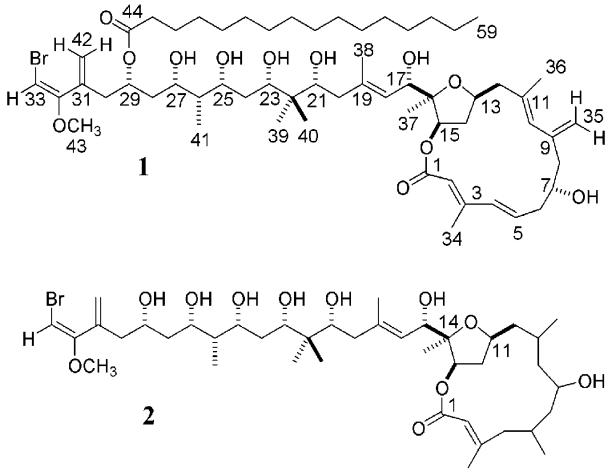

FIGURE 1. Structures of phormidolide (**1**) and oscillariolide (**2**).

cultures and was found to possess potent brine shrimp toxicity (LC_{50} = 1.5 μM). Preliminary NMR analysis showed it to be of an extremely complex molecular constitution. Herein, we report on the isolation and structure elucidation, including absolute stereochemistry, of this new macrolide, phormidolide (**1**).

Results and Discussion

The structure of phormidolide was determined by a strategy that depended on a combination of spectroscopic techniques, principally NMR. Characterization of the planar structure of phormidolide (**1**, Figure 1) was carried out using a suite of 1- and 2-dimensional NMR techniques including 1D ^{1}H and ^{13}C NMR, DEPT,[7] GCOSY,[8] PEPHSQC,[9] pure absorption TOCSY,[10] GHMBC,[8] HSQMBC (heteronuclear single quantum multiple bond correlation),[11] GROESY,[12] INADEQUATE,[13] and a new ACCORD-ADEQUATE NMR experiment.[14] The relative stereochemistry was determined through the use of the *J*-based configuration analysis method[15] utilizing HSQMBC,[11] gradient-selected E.COSY,[16] and GROESY.[12] The absolute stereochemistry was determined using the variable-temperature MPA NMR method using a partially protected bis-acetonide derivative (**3**) of phormidolide (**1**).

Phormidolide (**1**) was isolated in 15−20% yield as a clear, colorless oil from the CH_2Cl_2/MeOH extract of aged cultures of *Phormidium* sp., collected originally from Sulawesi, Indonesia. The molecular formula of **1** was determined by HRFABMS to be $C_{59}H_{97}BrO_{12}$ (*m*/*z* of [M + Na]$^+$ at 1099.5833). Sharp infrared absorptions at 1713 and 1640 cm^{-1} suggested the presence of ester and conjugated ester carbonyls, respectively; the latter functionality was supported by UV absorptions at 270 nm. Additionally, multiple hydroxyl functionalities were indicated by a strong IR absorption centered at 3404 cm^{-1}, and an additional conjugated diene was suggested from UV absorption at 240 nm.

Several features of the NMR spectra suggested a polyketide-derived metabolite of possible macrocyclic structure. Readily observed from the 1D ^{13}C NMR and DEPT experiments were nine methyl carbon atoms, 22 high-field methylene carbons, one high-field methine carbon, and one high-field quaternary carbon atom. Additionally, these spectra revealed the presence of seven protonated olefinic carbons, one additional protonated olefinic carbon attached to a highly shielding substituent, six quaternary olefin carbons, two ester carbonyls, nine oxymethine carbons, and one quaternary carbinol carbon. Inherent to this molecular formula are 11 degrees of unsaturation; as the above carbon inventory explains the nature of nine of these, phormidolide (**1**) was deduced to be bicyclic.

Analysis of the ^{1}H and ^{13}C NMR chemical shift data, ^{1}H−^{1}H coupling constants, magnitude-mode GCOSY,[8] PEP-HSQC[9] and HSQC-TOCSY,[10] and GHMBC,[8] along with comparison with data for the previously reported metabolite oscillariolide (**2**),[17] identified the 13 partial structures shown in Figure 2, parts A−M. For example, in partial structure B, a trans-disubstituted olefin was shown by COSY to be sequentially correlated to adjacent methylene, oxymethine, and methylene groups. Similarly, a series of alternating oxymethines and high field methylene or methine groups were characterized in partial structure J. At one end of this partial structure (C-29), the oxymethine was considerably deshielded (δ 5.0) compared to the other oxymethines (δ3.65−4.08), consistent with its presence as an ester. An alternation of oxymethines and high field methylene groups was characterized in partial structure E as well (CH_2-12 at δ48.3 next to CH-13 at δ76.7 next to CH_2-14 at δ34.8 next to CH-15 at δ79.6). In partial structure G, a vinyl proton at δ5.40 (C-18) was vicinally coupled to an oxymethine at δ4.70 (C-17) and allylically coupled to a vinyl methyl group at δ1.80 (C-38).

Partial structure M was easily assigned to a saturated fatty acyl chain; however, NMR analysis alone was not able to establish its chain length. This was determined by microwave-catalyzed trans-esterification in 1 M HCl/MeOH and analysis of the resultant methyl ester by GC−MS.[18] A single peak was observed which was identical

(6) Singh, I. P.; Boulanger, A. B.; Marquez, B.; France, D.; Bair, K. W.; Gerwick, W. H. *J. Nat. Prod*. in prep.
(7) Doddrell, D. M.; Pegg, D. T.; Bendall, M. R. *J. Magn. Reson*. **1982**, *48*, 323−327.
(8) Willker, W.; Leibfritz, D.; Kerssebaum, R.; Bermel, W. *Magn. Reson. Chem*. **1993**, *131*, 287−292.
(9) Schleucher, J.; Schwendinger, M.; Sattler, M.; Schmidt, P.; Schedletzky, O.; Glaser, S. J.; Sorensen, O. W.; Griesinger, C. J. *Biomol. NMR* **1994**, *4*, 301−306.
(10) Kover, K. E.; Uhrin, D.; Hruby, V. J. *J. Magn. Reson*. **1998**, *130*, 162−168.
(11) Williamson, R. T.; Marquez, B. L.; Gerwick, W. H.; Kover, K. E. *Magn. Reson. Chem*. **2000**, *38*, 265−273.
(12) Parella, T.; Sanchez-Ferrando, F.; Virgili, A. *J. Magn. Reson*. **1998**, *135*, 50−53.
(13) Bax, A.; Freeman, R.; Frenkiel, T. A.; Levitt, M. H. *J. Magn. Reson*. **1980**, *43*, 478−450.
(14) (a) Reif, B.; Koeck, M.; Kerssebaum, R.; Kang, H.; Fenical, W.; Griesinger, C. *J. Magn. Reson. Ser. A* **1996**, *118*, 282−285. (b) Williamson, R. T.; Marquez, B. L.; Gerwick, W. H.; Koehn, F. E. *Magn. Reson. Chem*. **2001**, *39*, 544−548.
(15) (a) Murata, M.; Matsuoka, S.; Matsumori, N.; Paul, G. P.; Tachibana, K. *J. Am. Chem. Soc*. **1999**, *121*, 870−871. (b) Matsumori, N.; Kaneno, D.; Murata, M.; Nakamura, H.; Tachibana, K. *J. Org. Chem*. **1999**, *64*, 866−876.
(16) Willker, W.; Leibfritz, D.; Kerssebaum, R.; Lohman, J. *J. Magn. Reson. Ser. A*. **1993**, *102*, 348−350.
(17) Murakami, M.; Matsuda, H.; Makabe, K.; Yamaguchi, K. *Tetrahedron Lett*. **1991**, *32*, 2391−2394.
(18) Williamson, R. T. Masters Thesis, University of North Carolina at Wilmington, 1996.

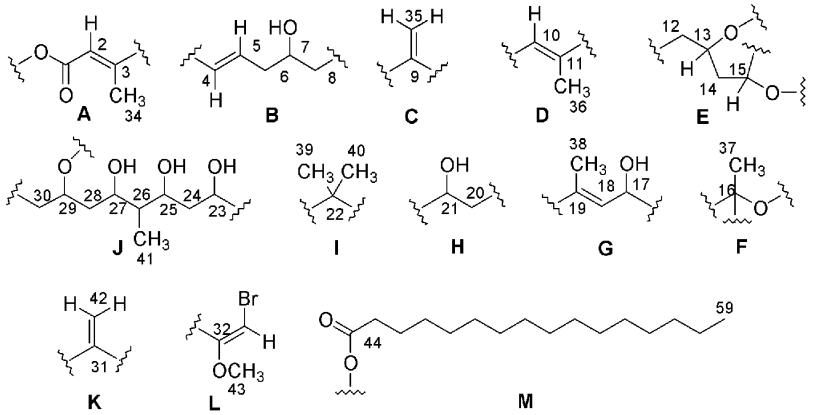

FIGURE 2. Partial structures A−M determined for phormidolide (**1**) from ^{1}H−^{1}H coupling constant data, ^{1}H−^{1}H COSY, PEP-HSQC, PEP-HSQC-TOCSY, and GHMBC experiments.

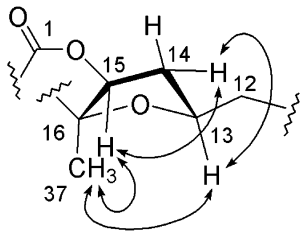

FIGURE 3. Key ROE and NOE correlations for protons about the tetrahydrofuran ring of phormidolide (**1**).

in retention time and fragmentation pattern with methyl palmitate. GHMBC cross-peaks between the C-43 methoxy group and C-32, as well as between H-33 and C-32, placed a methoxy group on an unusually polarized olefinic bond (C-32 δ 158.4, C-33 δ 78.8). Comparison of these data with that reported for oscillariolide,[17] as well as consideration of the molecular formula, led to formulation of partial structure L as a methyl-trapped enol ether with vinyl bromide functionality. Similar NMR arguments were utilized to establish the remainder of the partial structures in phormidolide, and collectively, accounted for all carbon and oxygen atoms in phormidolide (two ester oxygens were redundantly identified in this analysis).

Connections between these partial structures were made through the use of GHMBC[8] and GROESY[12] experiments. Cross-peaks in the GHMBC spectrum from H-2 to C-1, C-3, C-4, and C-34, and from H-4 to C-2 and C-3, allowed connection of partial structures A and B (Figure 2). The other end of partial structure B, H_2-8, showed correlations to C-35, C-9, and C-10, revealing the placement of an *exo*-methylene group (C) between C-8 and C-10. In turn, H-10 showed GHMBC correlations to C-9, C-35, C-8, C-12, and C-36, confirming placement of this *exo*-methylene moiety between partial structures B and D. Additional GHMBC correlations from H-12 to C-36, C-11, and C-10 reiterated this connection as well as formed a link between partial structures D and E.

The existence of a tetrahydrofuran ring in phormidolide (**1**), as well as the connection between partial structures E and F, was initially revealed by a ROESY correlation from H-13 to H_3-37 (Figure 3). Analogous with structural studies on oscillariolide A,[17] a GHMBC correlation (8 Hz optimization) was not observed between H-13 and C-16 in phormidolide. However, GROESY correlations along with chemical shift comparisons to oscillariolide (**2**)[17] supported this spatial arrangement. Confirmation was obtained by observing a 10.6 Hz coupling between H-13 and C-16 as detected by 2D HSQMBC. Additionally, GHMBC showed correlations from H-15 to C-16, C-17, and C-37, firmly tying together partial structures E, F, and G and substantiating the tetrahydrofuran ring. A connection between the tetrahydrofuran ring and partial structure A was established by a strong GHMBC correlation from H-15 and the ester carbonyl C-1, thus forming a 16-membered lactone ring.

The connection between partial structure G and H was demonstrated bi-directionally by correlations from H-18 to C-20 and C-38 and from H-20a to C-18, C-19, and C-38. The placement of a geminal dimethyl group (partial structure I) between structure H and J was shown by GHMBC correlations from H_3-39 and H_3-40 to C-21, C-22, and C-23. As noted above, the distinctive ^{1}H and ^{13}C shifts of C-29 versus those at C-27, C-25, C-23, and C-21 (Table 1) indicated that an ester group was attached at this position. A GHMBC correlation between the H-29 proton and ester carbonyl at δ 173.7 confirmed this assignment. GHMBC correlations from H-45 to C-44, C-46 and the overlapped methylene envelope at 30 ppm additionally confirmed the presence of this fatty acyl chain.

The methylene protons at H_2-30 showed correlations to C-31, whereas the exo-methylene protons (H_2-40) showed correlations to C-31 as well as C-30 and C-32, thereby placing the second *exo*-methylene group (partial structure K) between partial structure J and a terminating partial structure L. These connections between partial structures A−L completed the initial hypothesis concerning phormidolide's planar structure; this was confirmed by INADEQUATE analysis of a ^{13}C-enriched sample of phormidolide as described below.

A ^{13}C-enriched sample of phormidolide was prepared by culturing the producing *Phormidium* sp. in medium supplemented with [1,2-$^{13}C_2$]acetate. A robust ^{13}C incorporation was achieved into phormidolide (ca. 6%), which was then analyzed by the INADEQUATE pulse sequence.[13] Under the conditions of this ^{13}C-incorporation experiment, a number of endogenously produced metabolic precursors to phormidolide became enriched from the ^{13}C source, presumably from metabolism of the acetate label and re-incorporation of the released CO_2 via

TABLE 1. NMR Data Used To Determine the Planar Structure of Phormidolide (1)[a,b]

carbon	δ_C, multiplicity	δ_H, multiplicity (Hz)	GCOSY	GHMBC
1	167.5, s			
2	118.3, d	5.80, s	H: 34	1, 3, 4, 34
3	152.1, s			
4	134.1, d	6.20, d (15.8)	H: 5, 6 (2.85)	2, 3, 6, 7, 34
5	132.6, d	5.88, ddd (15.8, 11.8, 3.9)	H: 4, 6 (2.85)	3, 6, 7
6	44.1, t	2.85, ddd (11.8, 3.9, 3.9)	H: 4, 6 (2.13), 7	4, 5, 7, 8
		2.13, ddd (11.8, 11.8, 10.5)	H: 6 (2.85), 5, 7	4, 5, 7, 8
7	73.1, d	4.05, dddd (10.5, 10.5, 3.9, 3.9)	H: 6, 7	
8	43.8, t	2.46, bd (14.8)	H: 7, 35	7, 9
		1.81, ovlp	H: 7, 35	6, 7, 9, 10, 35
9	141.5, s			
10	132.4, d	5.28, bs		8, 12, 35, 36
11	133.4, s			
12	48.3, t	2.33, ovlp	H: 12 (2.58), 13	10, 11, 13, 14, 36
		2.58, ovlp	H: 12 (2.33), 13, 10	10, 11, 13, 14
13	76.7, d	4.48, m	H: 12, 14	15, 16
14	34.8, t	1.57, ovlp	H:13, 14 (2.33), 15	12, 15, 16
		2.33, ovlp	H: 13, 14 (1.57), 15	12, 13
15	79.6, d	5.15, d (4.8)	H: 14	1, 13, 16, 37
16	86.9, s			
17	69.7, d	4.70, d (9.0)	H: 18	15, 16, 18, 19, 37
18	127.0, d	5.40, ovlp	H: 17, 20 (2.34), 38	20, 38
19	137.4, s			
20	42.3, t	2.06, dd (13.1, 10.5)	H: 20 (2.34), 21	18, 19, 21, 22, 38
		2.34, ovlp	H: 18, 20 (2.06), 21, 38	18, 19
21	77.5, d	3.65, dd (10.5, 2.6)	H: 20	19, 22, 23, 40
22	40.4, s			
23	81.6, d	3.86, dd (10.5, 2.6)	H: 24	21, 24, 25, 40
24	35.1, t	1.65, m	H: 23, 24 (1.47), 25	22, 23, 25
		1.47, d (14.5)	H: 23, 24 (1.65), 25	
25	77.8, d	4.08, d (10.5)	H: 24, 26	23, 27, 41
26	41.5, d	1.49, m	H: 25, 27, 41	41
27	73.8, d	3.97, dd (6.6)	H: 26, 28	25, 28, 29, 41
28	39.2, d	1.76/1.76 ovlp	H: 27, 29	26, 27, 29, 30
29	70.5, d	5.0, ovlp	H: 28, 30	27, 28, 30, 31, 44
30	39.3, t	2.57, m/2.57, m	H: 29, 42	28, 29, 31, 32
31	138.3, s			
32	158.4, s			
33	78.8, d	5.33, s		31, 32, 42
34	13.9, q	2.07, s	H: 2	1, 2, 3, 4
35	113.8, t	4.76, bs	H: 8, 10	8, 10
		4.98, ovlp	H: 8	8, 9,10
36	16.8, q	1.58, s	H: 10	9, 10, 12
37	21.0, q	1.19, s		15, 16
38	17.3, q	1.80, s	H: 18, 20 (2.34)	18, 19, 20
39	13.7, q	0.91, s		21, 22, 23
40	21.6, q	0.74, s		21, 22, 23, 39
41	5.0, q	0.92 d (6.6)	H: 26	25, 26
42	122.1, t	5.37, s	H: 30	29, 30, 31, 32
		5.42, ovlp	H: 30	29, 30, 31, 32, 33
43	55.6, q	3.59, s		32, 33
44	173.7, s			
45	34.6, t	2.27/2.27 ovlp	H: 46	44, 46, 47−56
46	24.9, t	1.61/1.61 ovlp	H: 47−56	45, 47−56
47−56	29.7, t	1.25/1.25 ovlp	H: 46	47−56, 58
57	22.7, t	1.30/1.30 ovlp		47−56, 58
58	31.9, t	1.25/1.25 ovlp	H: 59	47−56, 57
59	14.1, q	0.87, t	H: 58	57, 58

[a] Data obtained on a Bruker 600 MHz instrument in $CDCl_3$. [b] ovlp = overlapped signals.

photosynthesis. This ^{13}C incorporation pattern allowed direct visualization of the connections between almost all adjacent carbon atoms in phormidolide by the standard pulse sequence (only the C-2−C-3, C-10−C-11, C-16−C-17, C-20−C-21, and C-24−C-25 connections were not clearly observed) (Figure 4). To detect these latter connectivities, a new ACCORD-ADEQUATE pulse sequence was devised which optimizes for a range of homonuclear $^{13}C-^{13}C$ coupling constants (30−55 Hz). This allowed inverse detection of these remaining ^{13}C-^{13}C pairs with great sensitivity.[14b] These data obtained with ^{13}C-labeled **1** in concert with those described above firmly established the planar structure of phormidolide.

The relative stereochemistry of phormidolide was deciphered from a combination of homonuclear and heteronuclear coupling constants, NOE information from the GROESY experiment, and a key bis-acetonide derivative. The *E* geometry of the C-2−C-3 double bond was established from measurement of a large $^3J_{CH}$ (8.8 Hz) from H-2 to C-34 and strong NOE from H-2 to H-4. A 4(*E*) double bond was also indicated from the large $^3J_{HH}$ (15.8 Hz) between these protons and observation of NOE

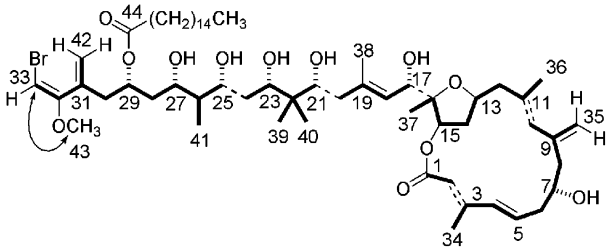

FIGURE 4. Overview of the $^{13}C-^{13}C$ couplings in ^{13}C-enriched phormidolide. Bold lines indicate $^{13}C-^{13}C$-coupled partners observed by the INADEQUATE NMR experiment optimized for a 45 Hz $^{13}C-^{13}C$ coupling constant. Dashed lines indicated additional key $^{13}C-^{13}C$ couplings observed using an ACCORD-ADEQUATE experiment (30−55 Hz optimization). The arrow from C-43 to C-33 indicates an observed long-range $^{13}C-^{13}C$ coupling of approximately 8 Hz.

between H-5 and H_3-34. ROE correlations from H-10 to H_2-12 and H_3-36 to H_2-35, as well as $^3J_{CH} = 8.1$ Hz between H-10 and C-36 and $^3J_{CH} = 7.0$ Hz between H-10 and C-12, demonstrated the *E* configuration of the C-10-C-11 olefin. The C-18−C-19 olefin was also shown to be *E* by virtue of ROE correlations between H-18 and H-20a and H_3-38 and H-17. This was confirmed from three-bond heteronuclear coupling data ($^3J_{H\text{-}18-C\text{-}38} = 10.0$ Hz and $^3J_{H\text{-}18-C\text{-}20} = 6.0$ Hz). Last, ROE correlations between the methoxy group H_3-43 and vinylic proton H-33 showed that the terminal bromine-containing double bond was also in the *E* configuration.

The relative stereochemistry of substituents about the tetrahydrofuran ring was determined using ROESY and selective 1D DPFGSE-NOE experiments.[19] Through space interactions were observed between H-13 and H_3-37, H-13 and H-14b, H-14b and H-15, and H-15 and H_3-37 (Figure 3). These NOEs clearly indicated that phormidolide had the same relative stereoconfiguration about these centers as oscillariolide (**2**).[17]

The relative configuration of the polyol chain was assigned using the recently reported *J*-based configuration analysis method developed by Murata and Tachibana.[15] This method utilizes the angular and substituent dependence of the homonuclear and heteronuclear coupling constant, expressable by a Karplus-type equation.[20,21] The method assumes that acyclic systems will exist in a series of staggered rotamers that can be deduced by the magnitude of these coupling constants

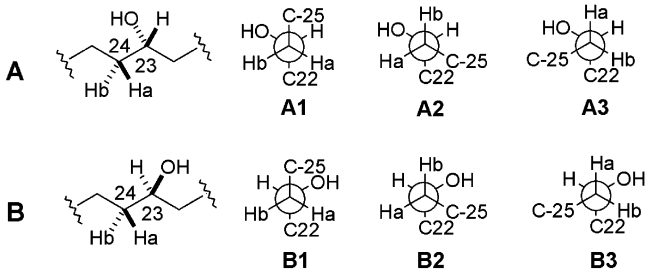

FIGURE 6. Diagram of all possible rotamers for the two possible diasterotopic orientations (A and B series) between C-23 and C-24.

in combination with NOE data. Because many of the protons of the polyol chain in phormidolide were overlapped, measurement of homonuclear coupling data was achieved utilizing the gradient selected E.COSY experiment.[16] Heteronuclear couplings were accurately and efficiently measured utilizing a newly created variant of the HSQMBC[11] experiment which we term here as the G-BIRD$_R$-HSQMBC NMR experiment (Figure 5).

This new method for determining heteronuclear coupling constants overcomes most of the problems encountered with the HETLOC[22] and phase-sensitive HMBC (psHMBC)[23] experiments. These problems include low sensitivity and complications due to the evolution of homonuclear couplings in the psHMBC.[23] A description of how these complications are overcome and circumvented with the HSQMBC pulse sequence has been published recently.[11] A clear advantage of the HSQMBC experiment is that only a single data set is required to accurately determine long-range heteronuclear coupling constants. Here we demonstrate the robust sensitivity of this new HSQMBC experiment by recording and measuring all coupling constants on a 15 mg sample of phormidolide (**1**) at natural isotopic abundance (ca. 28 mM).

The analysis of relative stereochemistry at C-23 and C-24 is described below as an example of the *J*-based configuration analysis applied to phormidolide (Figure 6). From E.COSY data, a $^1H-^1H$ coupling constant of 2.6 Hz between H-23 and H-24a suggested a gauche relationship between these two protons (e.g., Figure 6A1, 6A3, 6B2, or 6B3). Similarly, a $^1H-^1H$ coupling constant of 10.6 Hz between H-23 and H-24b indicated an anti relationship of these protons (e.g., Figure 6A1 or 6B3).

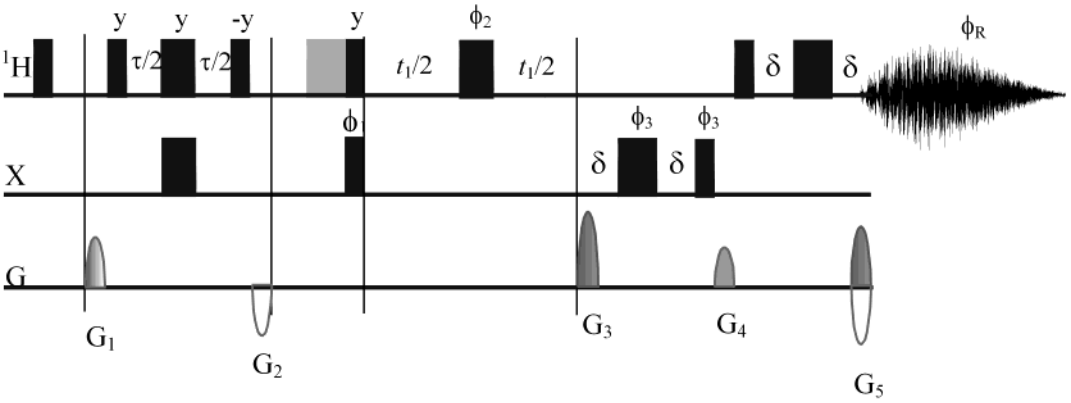

FIGURE 5. Pulse sequence of the G-BIRD$_R$-HSQMBC NMR experiment.

TABLE 2. NMR Data Used To Determine the Relative Stereochemistry of Phormidolide (1)[a,b]

carbon	δ_C, multiplicity	δ_H	ROESY	E.COSY (Hz)	HSQMBC (Hz)
1	167.5, s				
2	118.3, d	5.80	4, 10, 14b		34 (8.8), 4 (8.2)
3	152.1, s				
4	134.1, d	6.20	2, 6a, 10	5 (15.5)	6 (6.5), 34 (4.7), 2 (5.3)
5	132.6, d	5.88	6b, 34	6a (11.8), 6b (4.1), 4 (15.5)	7 (3.0), 3 (0.6)
6	44.1, t	2.85	8a, 4, 34	7 (10.5), 5 (11.8)	8 (2.1), 7 (8.3), 4 (2.0)
		2.13	7, 5	7 (2.3), 5 (4.1)	7 (2.3), 5 (4.1), 8 (8.0), 7 (7.3), 4 (0.9)
7	73.1, d	4.05	6b, 8b, 5, 35b	8a (11.5), 8b (2.3), 6a (10.5), 6b (4.0)	9 (<0.5), 5 (<0.5)
8	43.8, t	2.46	10	7 (11.5)	10 (2.0), 35 (3.5), 7 ovlp, 6 (4.0)
		1.81	7	7 (2.3)	10 (1.4), 35 (5.0), 7 (5.9), 6 (4.8)
9	141.5, s				
10	132.4, d	5.28	14b, 8a, 4, 2		36 (8.1), 12 (7.1), 35 (6.5), 8 (4.7)
11	133.4, s				
12	48.3, t	2.33		13 (14.0)	14 (<0.5), 10 (4.8), 36 (5.5)
		2.58	13, 36	13 (5.0)	14 (<0.5), 10 (3.0), 36 (2.8)
13	76.7, d	4.48	12b, 14b, 36, 37	14a (0.0), 14b ovlp, 12a (14.0), 12b (5.0)	11 (<0.5), 16 (10.6)
14	34.8, t	1.57	15	15 (0.0), 13 (0.0)	13 (<0.5), 12 (4.1)
		2.33	13, 15, 2	15 (4.8), 13 ovlp	13 (<0.5), 12 (4.5)
15	79.6, d	5.15	12a, 14a, 17 (st), 37 (wk), 18 (wk)	14a (0.0), 14b (4.8)	17 (<0.5), 37 (5.5)
16	86.9, s				
17	69.7, d	4.70	38 (st), 15 (st), 37 (wk)	18 (9.0)	19 (3.7), 16 (5.6), 15 (5.5), 37 (5.0)
18	127.0, d	5.40	37 (st), 20a, 15 (wk)	17 (9.0)	20 (6.0), 16 (0.8), 38 (10.0)
19	137.4, s				
20	42.3, t	2.06	18, 39	21 (10.6)	22 (0.4), 38 (6.3), 18 (6.5), 21 (2.0)
		2.34	21, 40, 38	21 (2.3)	18, 19
21	77.5, d	3.65	20b, 38, 40, 23	20a (10.6), 20b (2.4)	23 (2.0), 39 (5.0), 40 (0.8), 19 (3.5)
22	40.4, s				
23	81.6, d	3.86	24a, 25, 21, 40	24a(2.6), 24b (10.6)	39 (5.0), 40 (0.7), 21 (1.8)
24	35.1, t	1.65	25, 40, 23	25 (1.0), 23 (2.6),	25 (2.5), 23 (2.1), 22 (<0.5)
		1.47	39	25 (10.5), 23 (10.6)	26 (<0.5), 25 (5.5), 23 (6.0), 22 (<0.5)
25	77.8, d	4.08	24a, 26, 27, 23	26 (1.0), 24a (1.0), 24b (10.5)	27(0.6), 23 (0.9), 41 (10.0)
26	41.5, d	1.49	27, 25	27 (<1.0), 25 (2.9)	28 (<0.5), 27 (2.2), 25 (2.1), 24 (<0.5)
27	73.8, d	3.97	28a, 26, 25	28a (6.6), 28b (6.6), 26 (<1.0)	29 (3.2), 41 (4.0), 25 (2.8)
28	39.2, d	1.76	29, 26, 27, 42	29 (5.1), 27 (6.6)	26, 27, 29, and 30 ovlp
		1.79	41	29 (8.0), 27 (6.6)	26, 27, 29, and 30 ovlp
29	70.5, d	5.0	28a, 26, 27, 42		27, 28, 30, 31, 44
30	39.3, t	2.57		30a (6.5), 30b (10.0), 28a (5.1), 28b (8.0)	29 and 28 ovlp
		2.57		29 (6.5)	29 and 28 ovlp
31	138.3, s			29 (10.0)	
32	158.4, s				
33	78.8, d	5.33	43		31 (6.5)
34	13.9, q	2.07			1, 2, 3, 4
35	113.8, t	4.76	34, 36		10 (5.9), 8 (10.0)
		4.98	7		10 (11.2), 8 (5.9)
36	16.8, q	1.58	13, 35a		9, 10, 12
37	21.0, q	1.19	13, 17 (wk), 15, 18 (st)		15, 16
38	17.3, q	1.80	21, 17 (st), 20b		18, 19, 20
39	13.7, q	0.91	24b, 20a		21, 22, 23
40	21.6, q	0.74	21, 23, 24a, 20b		21, 22, 23, 39
41	5.0, q	0.92	28b, 24b		25, 26
42	122.1, t	5.37	29		
		5.42			
43	55.6, q	3.59	33		32, 33
44	173.7, s				
45	34.6, t	2.27			44, 46, 47−56
46	24.9, t	1.61			45, 47−56
47−56	29.7, t	1.25			47−56, 58
57	22.7, t	1.30			47−56, 58
58	31.9, t	1.25			47−56, 57
59	14.1, q	0.87			57, 58

[a] Data obtained on a Bruker 600 MHz instrument in $CDCl_3$. [b] Abbreviations used: wk = weak NOE, st = strong NOE, ovlp = overlapped signals.

Measurement of $^2J_{CH}$ coupling constants of 2.1 and 6.0 Hz between H-24a and C-23 and H-24b and C-23, respectively, indicated that H-24a was anti and H-24b was gauche to the electronegative oxygen substituent at C-23 (e.g., Figure 6A1 or 6B2). Finally, a $^3J_{CH}$ of <0.5 Hz between both H-24a and H-24b and C-22 indicated that both protons were gauche to this group; only rotamer A1 (or its enantiomer) meets all of these criteria and thus represents the relative configuration of these two centers. In a similar fashion, the relative stereochemistry was established for all stereocenters along the acyclic portion of phormidolide (C-20 to C-29) (Table 2 and Figure 7).

(19) Stott, K.; Keeler, J.; Van, Q. N.; Shaka, A. J. *J. Magn. Reson.* **1997**, *125*, 302−324.
(20) Barfield, M.; Smith, W. *J. Am. Chem. Soc.* **1992**, *114*, 1574−1581.
(21) Osawa, E.; Imai, K. *Magn. Reson. Chem.* **1990**, *28*, 668−674.
(22) Otting, G.; Wuthrich, K. *Quart. Rev. Biophys.* **1990**, *23*, 39−96.
(23) Zhu, G.; Renwick, A.; Bax, A. *J. Magn. Reson. Ser. A.* **1994**, *110*, 257−261.

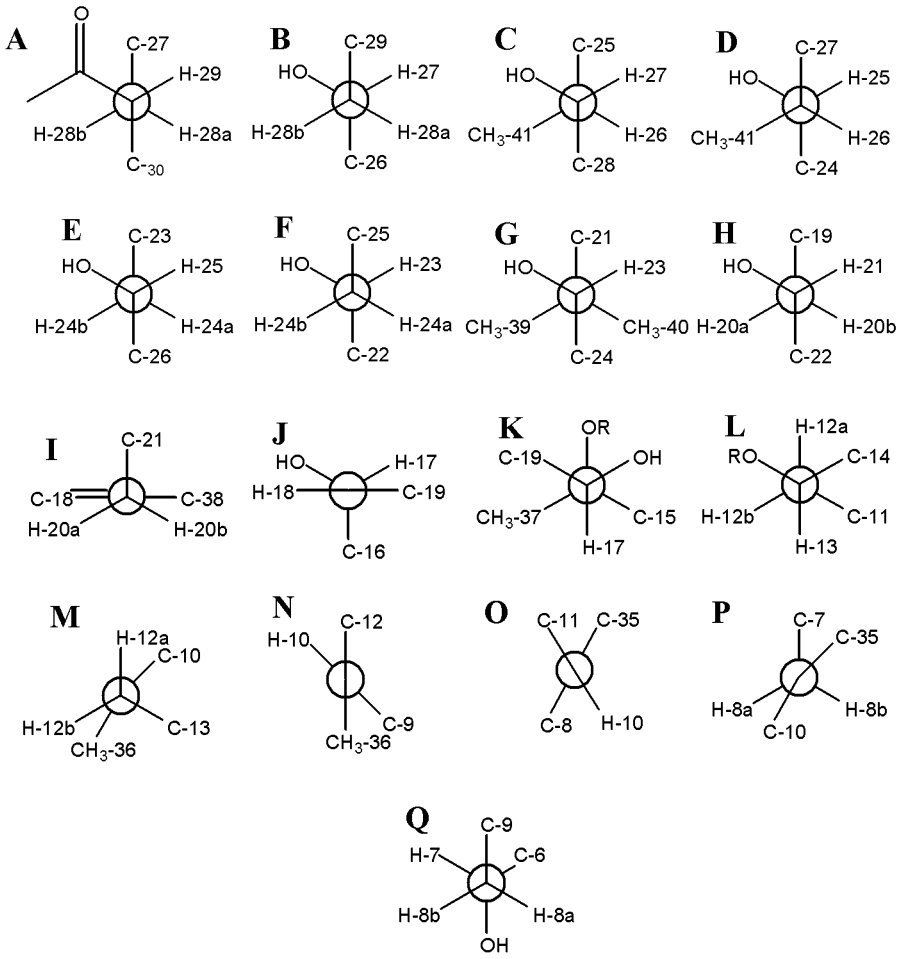

FIGURE 7. Diagram of the rotamers determined for phormidolide (**1**) using the *J*-based configuration analysis method and the data presented in Table 2.

An extension of *J*-based configuration analysis allowed connection of the relative stereochemistry at C-20 to that at C-17 and then on to the relative stereochemistry of the tetrahydrofuran ring and chiral centers within the macrolactone. The diastereotopic protons at C-20, which already had been related to the stereochemistry at C-21 (Figure 7H), could be related to the H-18 and H_3-38 orientations through strong dipolar coupling between H-20a and H-18 and H-20b and H_3-38 (Figure 7I). Large heteronuclear couplings (6−8 Hz) between both H-20a and C-18 and H-20b and C-38 substantiated this assignment. A small heteronuclear coupling from H-17 to C-19 (3.7 Hz), a large homonuclear coupling from H-17 to H-18 (9.0 Hz), and a very strong NOE from H-17 to H_3-38, required that H-17 and H-18 be placed in an anti relationship. A gauche relationship between H-17 and both C-15 and C-37 was indicated by similar magnitude heteronuclear couplings between this proton and both carbon atoms (5.5 and 5.0 Hz, respectively, Figure 7K). Relatively strong NOE correlations between H-18 and H_3-37 and H-17 and H-15 compared to very weak NOE correlations from H-17 to H_3-37 and H-18 to H-15 further confirmed the stereochemical assignment for this portion of the molecule. In turn, the relative stereochemistry of the tetrahydrofuran was established by NOE measurements, as described above.

A very large homonuclear coupling from H-13 to H-12a (14.0 Hz), an intermediate-sized homonuclear coupling from H-13 to H-12b (5.0 Hz), a small heteronuclear coupling from H-13 to C-11 (<2 Hz), and a strong ROE from H-13 to H-12b, supported the relative orientation depicted in Figure 7L. In turn, an *anti*-orientation between H-12a and C-36 was indicated from a relatively large heteronuclear $^3J_{\text{H-12a–C-36}}$ (5.5 Hz), a small $^3J_{\text{H-12b–C-36}}$ (2.8 Hz), and a strong ROE between H-12b and H_3-36 (Figure 7M). The anti relative orientation of H-10 and the exo-olefin was demonstrated by a large heteronuclear $^3J_{\text{H-10–C-35}}$ (6.5 Hz) and a strong ROE between H_3-36 and H_2-35 (Figure 8). The H-8b proton and C-35 CH_2 group were shown to be on the same face of the ring by virtue of an ROE interaction between them as well as a small $^3J_{\text{H-8b–C-35}}$ (3.5 Hz) and large $^3J_{\text{H–8a–C-35}}$ (5.0 Hz). Finally, large $^2J_{\text{H-8b–C-7}}$ (5.9 Hz) and small $^3J_{\text{H-7–C-9}}$ (<0.5 Hz) heteronuclear couplings, taken together with small $^3J_{\text{H-8a–H-7}}$ (2.3 Hz) and large $^3J_{\text{H-8b–H-7}}$ (11.5 Hz) homonuclear couplings, as well as an NOE between H-7 and H-8b, indicated the relative configuration depicted in Figure 7Q.

The absolute stereochemistry was established utilizing Mosher ester-type methodology on a partially derivatized form of phormidolide (**1**). Although various reaction conditions were employed, only the bis-acetonide **3** with

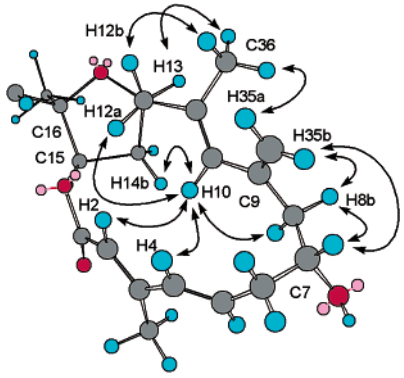

FIGURE 8. Key ROE correlations observed between protons of the macrolactone portion (C-1−C-16) of phormidolide (**1**). The model is aligned perpendicularly to the C-12−C-13 bond axis.

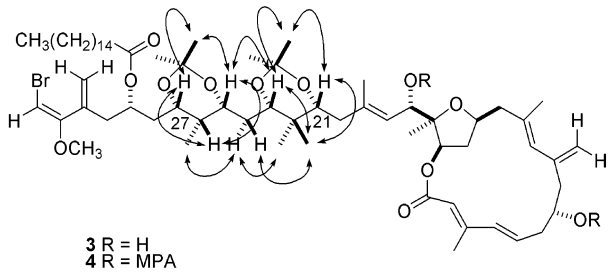

FIGURE 9. Phormidolide bis-acetonide derivatives **3** and **4** with key ROE correlations.

acetonides spanning the oxygens at C-21 and C-23, and C-25 and C-27, was obtained upon treatment of **1** with 2,2-dimethoxypropane and pyridinium-*p*-toluenesulfonic acid (Figure 9). An HSQC experiment of derivative **3** allowed determination of the ^{13}C NMR chemical shifts of the new methyl group resonances at approximately 19 and 30 ppm, a chemical shift difference between axial and equatorial methyl groups diagnostic (e.g., >10 ppm) for *syn*-acetonides (for trans acetonides, both methyl groups resonate at ca. 25 ppm).[24] Moreover, the syn configuration was further substantiated from strong NOE enhancements between the methine protons (H-21, H-23, H-25, and H-27) and the axial methyl groups, but not the equatorial methyl groups, of the two acetonides. Hence, the relative configurations deduced from the *J*-based configuration analysis at C-21 and C-23, and C-25 and C-27 (but not necessarily C-23 and C-25), were confirmed.

The bis-acetonide derivative **3** was derivatized with (*R*)-(−)-methoxyphenyl acetic acid using a standard DCC-catalyzed coupling reaction (Figure 9).[25] This derivative was chosen because of the larger induced chemical shifts in secondary alcohols relative to the MTPA derivative,[26] and it has been used previously in a variable temperature analysis that obviates the requirement of forming two diastereomeric derivatives.[27] Variable temperature analysis of derivative **4** and application of Mosher ester analysis revealed that the stereochemistry at C-7 is *R* (Figure 10). The additional ester formed at C-17 had no apparent effect on this analysis. As the relative stereochemistry of all stereocenters was already established, the absolute stereochemistry of phormidolide (**1**) was deduced as 7(*R*), 13(*S*), 15(*R*), 16(*R*), 17(*R*), 21(*R*), 23(*S*), 25(*R*), 26(*R*), 27(*S*), 29(*S*). Interestingly, this analysis agrees with the stereochemistry predicted by Celmer's rule for the stereochemical configuration of polyketide-type natural products.[28]

The substantial number of structural restraints provided by the combination of the homonuclear and heteronuclear coupling constants, along with the ROESY and NOE experiments, were used to direct a molecular modeling study of the three-dimensional structure of phormidolide (**1**). These restraints were entered into the Macromodel molecular modeling program[29] and used to define a lowest energy structure (Figure 11 and Experimental Section). It should be noted that these NMR restraints were developed from experiments run on phormidolide in $CDCl_3$, and hence, do not necessarily accurately depict its structure in biological systems. However, it is possible that phormidolide adopts a conformation similar to that obtained in this organic solvent when it is bound to lipophilic matrixes, including its putative biochemical target or receptor.

In conclusion, the planar and stereo structure of phormidolide has been determined by mainly NMR methods, making abundant use of the newly articulated *J*-based configuration analysis.[15] Phormidolide is an exceptional metabolite in its overall molecular size, 16-membered lactone ring, 11 stereogenic centers, and unique vinyl bromide functionality. The majority of phormidolide's structure appears to derive from polyketide metabolism; however, the metabolic origin of the starter unit which includes the vinyl bromide functionality is not obvious. Furthermore, phormidolide possesses a number of pendant carbon atoms, present either as methyl or exomethylene groups. Intriguingly, some of these are attached to what are logically derived from C-2 of acetate units whereas others are attached to carbons likely derived from C-1. Current efforts are examining the metabolic origins of these pendant atoms through isotope-labeled precursor feeding studies employing cultures of the phormidolide-producing *Phormidium*, and will be reported in due course. In biological screening, phormidolide was found to be a potent brine shrimp toxin (LD_{50} = 1.5 μM) but was not active in the NCI's in vitro 60-cell line toxicity assay.[30] As it is clear that this prokaryote expends considerable metabolic resources in the construction of phormidolide, it most certainly has an important adaptive significance, perhaps involving deterrence of predation.

(24) Rychnovsky, S. D.; Richardson, T. I.; Rogers, B. N. *J. Org. Chem.* **1997**, *62*, 2925−2934.
(25) Hoye, T.; Renner, M. K. *J. Org. Chem.* **1996**, *61*, 2056−2064.
(26) (a) Sullivan, G. R.; Dale, J. A.; Mosher, H. S. *J. Org. Chem.* **1973**, *38*, 2143-2147. (b) Trost, B. M.; Belletire, J. L.; Godleski, S.; McDougal, P. G.; Balkovec, J. M. *J. Org. Chem.* **1986**, *51*, 2370−2374. (c) Latypov, S. K.; Seco, J. M.; Riguera, R. *J. Org. Chem.* **1996**, *61*, 8569−8577.
(27) Latypov, S. K.; Seco, J. M.; Quiñoá, E.; Ricardo, R. *J. Am. Chem Soc.* **1998**, *120*, 877−882.
(28) (a) Celmer, W. D. *J. Am. Chem. Soc.* **1965**, *87*, 1801−1802. (b) Holzbauer, I. E.; Harris, R. C.; Bycroft, M.; Cortes, J.; Bisang, C.; Staunton, J.; Rudd, B. A.; Leadley, P. F. *Chem. Biol.* **1999**, *6*, 189−195.
(29) Macromodel 7.0; molecular modeling software, Schrodinger, Inc.; Portland OR, 1998.
(30) Stinson, S. F.; Alley, M. C.; Kopp, W. C.; Fiebig, H. H.; Mullendore, L. A.; Pittman, A. F.; Kenney, S.; Keller, J.; Boyd, M. R. *Anticancer Res.* **1992**, *12*, 1035−1053.

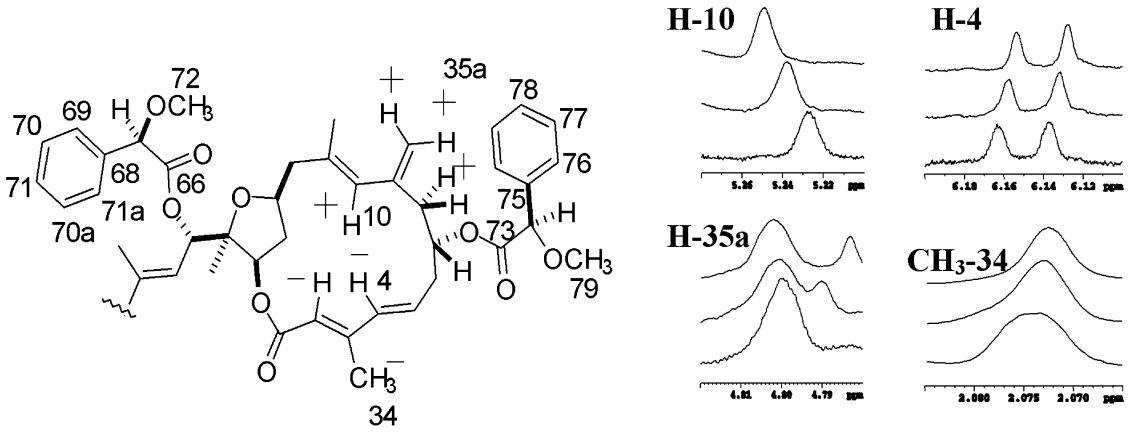

FIGURE 10. Results of a variable-temperature NMR study on the methoxyphenylacetate (MPA) derivative (**4**) of phormidolide bis-acetonide (**3**).

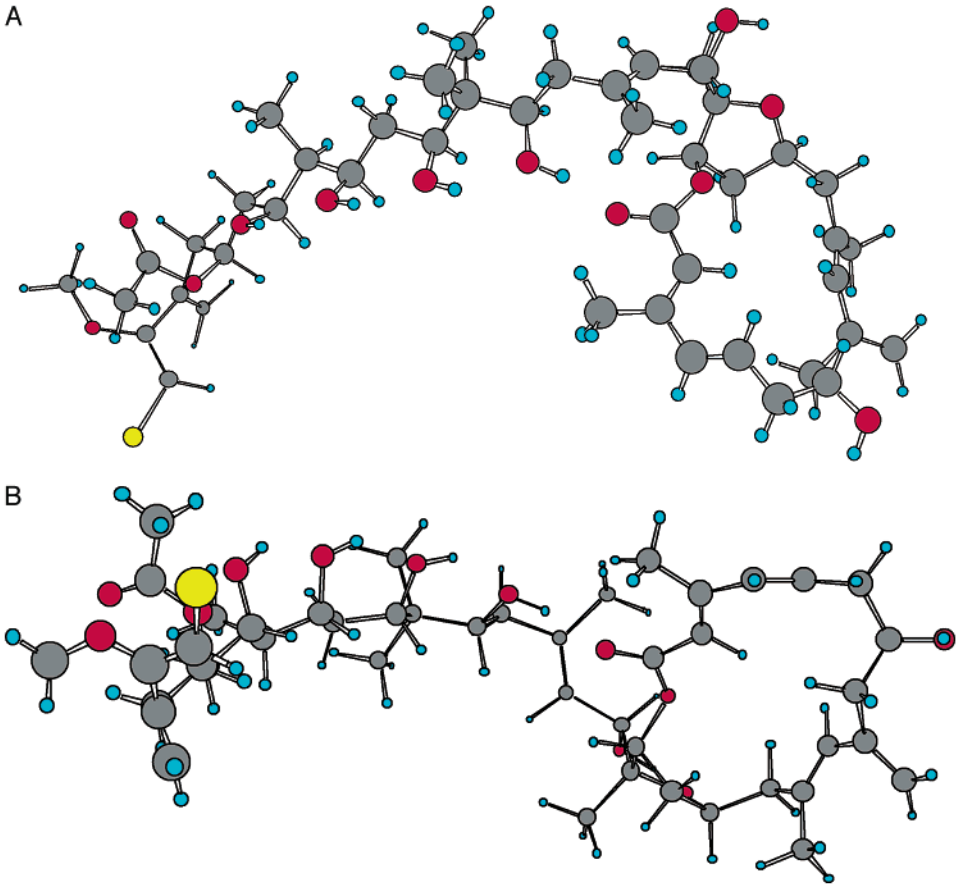

FIGURE 11. Three-dimensional structure of phormidolide (**1**) as determined from NMR-restrained molecular modeling using Macromodel: (a) top view and (b) bottom view (the fatty acyl group has been removed from this analysis).

Experimental Section

General Methods. Nuclear magnetic resonance (NMR) spectra were recorded on a Bruker DRX600 spectrometer operating at a proton resonance frequency of 600.01 MHz. Proton spectra were referenced to 7.26 ppm for residual $CHCl_3$. Carbon spectra were referenced to 77.0 ppm for $CDCl_3$. High-performance liquid chromatography (HPLC) utilized Waters M6000A or Waters 505 pumps, a Rheodyne 7125 injector, and a Waters Lambda-Max 480 LC spectrophotometer or Photodiode Array Detector model 996. Merck aluminum-backed thin-layer chromatography (TLC) sheets (silica gel 60_{F254}) were used for TLC analysis. Vacuum liquid chromatography (VLC) was performed with Merck silica gel G for TLC or with Baker bonded phase-ODS.

Culture Conditions. The original specimen of *Phormidium* sp. was obtained by scuba diving from Sulawesi, Indonesia (collection code ISB-3N94-8PLP; culture code HB3/1/21). The culture was inoculated into a 3 L Fernbach flask containing 1.5 L of artificial seawater SWBG11 medium and grown at 28 °C with a 16 h light/8h dark regimen for ~70 days before harvest.[31]

Isolation of Phormidolide. On several separate occasions, *Phormidium* sp. was harvested by filtration on Whatman 934-AH glass microfiber filters and blotted dry to afford 7−10 g of

wet biomass. The algal mat was repeatedly extracted with 2:1 CH_2Cl_2/MeOH to afford 150−200 mg extract. The extract was subjected to silica gel VLC using a range of solvent systems from 0 to 100% EtOAc/hexanes followed by MeOH wash. The fractions containing phormidolide (100% EtOAc) were combined and evaporated to dryness. The phormidolide enriched fraction was purified by NP-HPLC (Phenomenex Luna 10 μ silica, 2 × 250 mm × 4.6 mm) using hexanes−EtOAc−isopropyl alcohol (60/35/5) to afford pure phormidolide (10−20 mg), resulting in a yield of 7−15% relative to the crude extract.

Phormidolide (1) [hexadecanoic acid 1-(4-bromo-3-methoxy-2-methylenebut-3-enyl)-3,5,7,9,13-pentahydroxy-13-(9-hydroxy-5,13,17-trimethyl-11-methylene-3-oxo-2,16-dioxabicyclo[13.2.1]octadeca-4,6,12-trien-17-yl)-4,8,8,11-tetramethyltridec-11-enyl ester]: clear colorless oil; $[\alpha]^{25}_D = +48$ ($c = 0.25$, $CHCl_3$); λ_{max} 240 nm, 270 nm (log ϵ 4.2, 4.02); IR (neat) 3404, 3098, 2920, 2853, 1713, 1640, 1607, 1440, 1379, 1318, 1234, 1201, 1145, 1095, 1034, 967, 867, 756 cm^{-1}; ^1H and ^{13}C NMR data in Tables 1 and 2; LRFABMS (in 3-nba, positive ion) *m*/*z* 1101 (21), 1099 (19), 989 (1), 853 (2), 811 (2), 767 (1), 683 (2), 639 (2), 467 (4), 137 (100); HRFABMS *m*/*z* [M + Na]$^+$ 1099.5833 (calcd for $C_{59}H_{97}O_{12}BrNa$, 1099.6061).

Production of ^{13}C-Enriched Phormidolide (1). For the INADEQUATE NMR experiment, ^{13}C-enriched phormidolide was obtained by feeding 2 × 1.5 L cultures of *Phormidium* sp. with [1,2-$^{13}C_2$]acetate (10 mg/L) on days 21, 28, 35, 42, and 49 post-innoculation. The cultures were harvested on day 53 and **1** was purified as described above. For the 1,1-ADEQUATE NMR experiment, ^{13}C-enriched phormidolide was obtained by feeding 2 × 1.5 L cultures of *Phormidium* sp. with [1,2-$^{13}C_2$]-acetate (10 mg/L) on days 54, 56, and 58 post-innoculation. The cultures were harvested on day 61 and **1** was purified by VLC and HPLC as described above and its identity confirmed by ^1H and ^{13}C NMR spectral features.

Phormidolide Diacetonide (3). Phormidolide (7.0 mg, 6.5 μM) was dissolved in 1 mL of 2,2-dimethoxypropane and cooled to 0 °C. To this was added 4.2 mg of pyridinium-*p*-toluenesulfonic acid, and the reaction was allowed to proceed for 1 h and then quenched with 5% aqueous $NaHCO_3$. The solution was repetitively partitioned between CH_2Cl_2 and H_2O. The organic layers were combined and blown dry under argon. The residue (6.8 mg) was then subjected to normal-phase silica gel HPLC using 40% EtOAc/hexanes. Four components eluted with the major being the desired diacetonide **3** (3 mg, 2.6 μmol, 40% yield): HRFABMS *m*/*z* [M + Na]$^+$ 1179.6670 (calcd for $C_{65}H_{105}O_{12}BrNa$, 1179.6688).

Phormidolide Diacetonide MPA Ester (4). Phormidolide diacetonide (**3**, 2 mg, 1.7 μM) was dissolved in 500 μL of CH_2Cl_2, and 1.4 mg of (*R*)-(−)-methoxyphenyl acetic acid was added followed by 8 μL of dicyclohexylcarbodiimide (1.0 M solution in CH_2Cl_2). The reaction was allowed to proceed for 24 h at room temperature (25 °C). The reaction mixture was filtered through a Kimwipe plug to remove urea and applied to a 3 cm^3 silica gel Bond-Elut cartridge. The diacetonide-protected MPA ester was eluted with 50% EtOAc/hexanes, evaporated to dryness, and purified by reversed-phase ODS HPLC (100% MeOH) to provide the desired product (**4**, 0.5 mg, 0.34 μmol, 20% yield): HRFABMS *m*/*z* [M + Na]$^+$ 1775.7741 (calcd for $C_{83}H_{121}O_{16}BrNa$, 1775.7741).

Molecular Modeling. Monte Carlo conformational searching through MacroModel (ver. 7) was used to search the potential energy surface. A total of 1,000 conformations were generated and minimized using the MM2* force field with the generalized Born/surface area (GB/SA) $CDCl_3$ model. Multiple searches were carried out using different starting geometries as well as different ring-closure bond choices. For our system, we have determined that 1000 structures are sufficient to reproduce search convergence from different starting geometries. After minimization, a conformer was saved only if its steric energy was within 30 kJ/mol of the instant global minimum (lowest energy structure known during an incomplete conformational search) and did not duplicate a previously stored conformer. The structures were then analyzed to determine whether they violated any coupling constant or NOE data. This analysis led to a single structure that did not violate any of the above-described restraints (Figure 11).

Acknowledgment. We gratefully acknowledge the permission of the Indonesian government to make these microalgal collections and the National Cancer Institute for their support (CA 52955). We also acknowledge the OSU Biochemistry and Biophysics NMR Facility for use of the Bruker DRX600 NMR instrument (V. Hsu) and OSU Mass Spectrometry Facility (B. Arbogast).

Supporting Information Available: Copies of ^1H, ^{13}C, E.COSY, PEP-HSQC, GHMBC, TOCSY, GROESY, FAB-MS, and HSQMBC NMR data for **1** and select 1D and 2D NMR for derivatives **3** and **4**. This material is available free of charge via the Internet at http://pubs.acs.org.

JO020240S

(31) Rossi, J. V.; Roberts, M. A.; Yoo, H.-D.; Gerwick, W. H. *J. Appl. Phycol.* **1997**, *9*, 195−204.